

A FRACTURE MECHANICS BASED MODEL FOR JOINTS UNDER CYCLIC LOADING

Eric Puntel*, Gabriella Bolzon† and Victor E. Saouma ‡

May 16, 2006

Abstract

A generalized interface model for joints and cracks in quasi-brittle materials is formulated. The proposed model marries an existing fracture mechanics based one developed for monotonic loading of concrete with another frictional based model developed for the cyclic response of rock joints to address the (reverse) cyclic response of rough surfaces in the presence of cohesive stresses is correctly addressed. The properties of the model and its capability to capture several experimentally observed behaviors are shown by the numerical simulations performed.

This joint constitutive model is particularly suitable to simulate the seismic response of dam/rock joints subjected to seismic excitation, or of concrete joints under reverse cyclic loading.

in-print ASCE Journal of Engineering Mechanics

Introduction

Joint and interfaces, coupled with cohesive stresses, are present in many structures spanning well over six orders of magnitudes in size (from metallic polycrystals, ceramics to dams and tectonic faults). In all cases, one is confronted with an actual or potential displacement discontinuity where classical continuum mechanics fails to provide a solution, and very often these displacement discontinuities are precisely the main source of nonlinearity.

Depending on the field of study, these discontinuities assume different names: interface, crack, joint, fault or even artificially built joint. A civil engineering application where cracks abound are dams where, let aside AAR, they are the major source of nonlinearity. They are present along the rock/concrete

*Dipartimento di Georisorse e Territorio, Università di Udine, via Cotonificio 114, 33100 Udine, Italy. Formerly Ph.D. student at Dipartimento di Ingegneria Strutturale, Politecnico di Milano, P.zza Leonardo da Vinci 32, 20133 Milano, Italy. E-mail: eric.puntel@polimi.it

†Associate Professor, Dipartimento di Ingegneria Strutturale, Politecnico di Milano, P.zza Leonardo da Vinci 32, 20133 Milano, Italy. E-mail: gabriella.bolzon@polimi.it

‡Professor, Department of Civil, Environmental, and Architectural Engineering, University of Colorado, Engineering Center ECOT 441, UCB 429, Boulder, CO 80309; Visiting Professor, Dipartimento di Ingegneria Strutturale, Politecnico di Milano, P.zza Leonardo da Vinci 32, 20133 Milano, Italy. E-mail: saouma@civil.colorado.edu

interface, lift joints, cantilever joints (with or without shear keys), in plain concrete cracks, or rock joints. Yet, irrespective of their origin, all those cracks can be correctly modelled by the same generalized model provided material parameters are appropriately set. Other civil structures where joints or cracks can be of particular concern are nuclear containment vessels, (Hansen and Saouma 2003). Surprisingly, interface elements have also been used, albeit at a much smaller scale, for improved understanding of ceramics (Saouma, Natekar and Sbaizero 2002), and aluminum (Iesulauro, Ingraffea, Arwade and Wawrzynek 2002).

Ever since the pioneering work of Goodman, Taylor and Brekke (1968), numerous joint or interface laws have been proposed for both discrete and smeared crack models in concrete structures, (Hohberg 1992).

Of particular interest to dam engineering are the models of Fenves, Mojtahedi and Reimer (1992), Divoux, Bourdarot and Boulon (1997), Hall (1998), and Ahmadi, Izadinia and Bachmann (2001). Each of those models indeed presents an innovative component, but none appears to have been generalized to account for many phenomena associated with reverse cyclic load, asperity degradation, softening of tensile strength and cohesion, or stiffness degradation.

Some mixed-mode interface models exploit the analogy with the mechanics of irreversible plastic processes to account for unrecoverable joint opening and sliding; to them belongs the proposal made by Plesha (1987) and several successive works based on it. The frictional behaviour of the joint under reversed shear in compression is mainly considered in this approach, widely used in rock mechanics.

Insight and deeper understanding of lower scale surface interactions can be achieved through micro-mechanics based models such as (Fox, Kana and Hsiung 1998), (Grasselli, Wirth and Egger 2002), Misra (2002). The prediction of the joint behaviour results from a statistical description of the surface topography, but this kind of information is seldom available to practical purposes in structural design and overall analysis. In these cases, phenomenologically based models, unburdened by mechanics, often result in easier modelling of experimental results, (Bažant and Gambarova 1980) (Divoux, Boulon and Bourdarot 1997).

Fracture mechanics based models set in an elasto-plasticity framework seem to be the most general formulation in terms of the range of problems they can address; see, e.g.: (Lotfi and Shing 1994), (Carol, Prat and López 1997), (Červenka, Kishen and Saouma 1998), and (Cocchetti, Maier and Shen 2002). In particular, they permit to include and follow strength deterioration leading to the formation and progressive development of natural joints (i.e., cracks).

To the best of the authors' knowledge, the only generalized model addressing cyclic load, though in a displacement based formulation, is the one of Giambanco and Di Gati (1997) based on previous frictional-dilatant models by Snyman and Martin (1992) and Mróz and Giambanco (1996). The model, intended for the structural analysis of masonry blocks, introduces a piece-wise linear yield condition governed

by two independent internal variables. In the present model a unique yield function is defined and its evolution in the stress space controlled by a quantity which has a clear mechanical meaning, namely by a norm of inelastic displacement discontinuities. Moreover the present proposal is also different in the definition of roughness characteristics, e.g. through dilatant displacement and not dilatancy angle, and in their connection with the mechanical properties.

In this paper, an existing fracture mechanics based joint model, (Červenka et al. 1998), is extensively modified to account for cyclic loading (and accompanying surface degradation) in a manner similar to the one proposed by Plesha (1987). A suitable idealisation of the joint surface geometry is introduced for describing the macroscopic (overall) behaviour of the joint, more than for reflecting its microscopic structure as in (Fox et al. 1998), (Grasselli et al. 2002), Misra (2002).

A review of the monotonic interface element being extended is summarized first, then the formulation for cyclic load is presented. Finally the response of the generalized model at material point level is analyzed through a comparison with the model of Červenka et al. (1998) and with the cyclic shear experimental results of Kutter and Weissbach (1980).

The formulation presented herein is restricted to two dimensional situations; extension to 3D cases is conceptually straightforward only if isotropy is assumed in the joint plane.

Cyclic behavior of quasi brittle interfaces

Experimental studies on the cyclic behavior of quasi-brittle interfaces have been reported for both concrete and rock. For concrete they are mainly motivated by the investigation of the aggregate interlock phenomenon in which a slightly opened crack is subjected to reversed cyclic slip at given initial confinement, (Paulay and Loeber 1974), (Tassios and Vintzēleou 1987) and (Fronteddu, Léger and Tinawi 1998).

Numerous experiments on rock joints have been carried out. Of particular relevance to the present investigation is the work of Hutson and Dowding (1990), Lee, Park, Cho and You (2001), Homand, Belem and Souley (2001), and Jafari, Hosseini, Pellet, Boulon and Buzzi (2003). All of these studies contain also proposals of shear strength or dilatancy degradation laws derived from the tests.

In rock mechanics, a clear distinction is often made between first and second order asperities as those factors have a strong influence on joint response, (Patton 1966). First order asperities (from here on referred to as “asperities” unless otherwise noted) are associated with roughness of larger amplitude and wave-length and thus they tend to dominate dilatant behavior; second order asperities are associated with smaller amplitude and wave-length surface variations and are primarily responsible for the frictional forces exchanged along the inclined sliding surfaces.

In the case of a smooth joint, i.e. with no relevant first order asperities effects, the quasi-static response is characterized by almost no dilatancy and constant shear stress. This behavior can be captured

by a relatively simple non associate Coulomb type frictional law.

On the other hand, in rough joints (characterized by prominent first order asperities) the response depends on the slip direction (forward or backward). Mathematically, forward and backward slip are respectively defined as having an increasing or decreasing absolute value of tangential relative displacement.

In forward slip, not only does a rough joint dilate, but its apparent shear strength is also higher. The opposite is true for backward slip. Furthermore, both of these behaviors are affected by the degradation of the joint surfaces with progressive cycling: the dilatancy angle and the configurational difference in shear strength decrease as asperities are worn out.

Several models for rough interfaces have been published. A particularly effective mechanical interpretation was given by Plesha (1987), who assumed that sliding does not occur parallel to the joint mid-plane but along an inclined angle characterizing the asperities. Hence, writing the Coulomb slip criterion along the inclined slope, and expressing it in terms of joint stress vector components, the essential characteristics of backward and forward slip are captured.

The observed degradation of the joint characteristics with cycling loading is usually ascribed to the decrease of the asperity angle, often exponentially with the tangential work performed. This assumption, herein adopted, has been followed by Hutson and Dowding (1990), Qiu, Plesha, Huang and Haimson (1993), and Stupkiewicz and Mróz (2001).

Červenka 1994 hyperbolic model

Following a broad literature survey, (Puntel 2004), it was determined that the most suitable monotonic interface element for cyclic extension to the present dam-engineering oriented purpose, is the one originally developed by Červenka (1994) and subsequently published by (Červenka et al. 1998).

The formulation developed herein is two dimensional (2D), nevertheless the extension to the 3D case is straightforward provided that isotropy is assumed in the joint plane. Tractions and discontinuities considered are then 2D vectors with a normal and a single tangential component, referred to by subscript n and t respectively.

The strength (alias yield or activation) criterion of the interface is hyperbolic as also assumed by Carol et al. (1997), Lotfi and Shing (1994).

$$\varphi = p_t^2 - (c - p_n \mu)^2 + (c - \chi \mu)^2 \quad (1)$$

Three parameters define the interface strength: the two static internal variables, namely tensile strength χ and cohesion c , and the friction coefficient μ . The former two decrease bi-linearly with the effective inelastic displacement w^{ieff} which is the model's softening variable.

$$\chi(w^{\text{ieff}}) = \begin{cases} \chi_0 - \frac{\chi_0 - \chi_1}{w_{\chi_1}} w^{\text{ieff}} & 0 \leq w^{\text{ieff}} \leq w_{\chi_1} \\ \chi_1 \frac{w_{\chi_0} - w^{\text{ieff}}}{w_{\chi_0} - w_{\chi_1}} & w_{\chi_1} \leq w^{\text{ieff}} \leq w_{\chi_0} \end{cases} \quad (2)$$

$$c(w^{\text{ieff}}) = \begin{cases} c_0 - \frac{c_0 - c_1}{w_{c_1}} w^{\text{ieff}} & 0 \leq w^{\text{ieff}} \leq w_{c_1} \\ c_1 \frac{w_{c_0} - w^{\text{ieff}}}{w_{c_0} - w_{c_1}} & w_{c_1} \leq w^{\text{ieff}} \leq w_{c_0} \end{cases} \quad (3)$$

$$w_{\chi_0} = (2 G_f^I - \chi_0 w_{\chi_1}) / \chi_1 \quad (4)$$

$$w_{c_0} = (2 G_f^{IIa} - c_0 w_{c_1}) / c_1 \quad (5)$$

where: χ_0 , c_0 , G_f^I , G_f^{IIa} , w_{χ_1} , χ_1 , w_{c_1} , c_1 , w_{χ_0} , w_{c_0} are the material parameters described in the notation list.

Of these ten parameters, only eight are independent to define the bilinear curves; the other two (w_{χ_0} and w_{c_0}) can be determined from equations 4 and 5.

The rate of w^{ieff} is defined as the norm of the rate of inelastic displacements $\dot{\mathbf{w}}^i$:

$$\dot{w}^{\text{ieff}} = \|\dot{\mathbf{w}}^i\| = \left((\dot{w}_n^i)^2 + (\dot{w}_t^i)^2 \right)^{1/2} \quad (6)$$

The inelastic displacements $\dot{\mathbf{w}}^i$ are the sum of plastic (i.e. unrecoverable) and fracture (i.e. recoverable in tension only) displacements $\dot{\mathbf{w}}^p$ and $\dot{\mathbf{w}}^f$ respectively; total displacement discontinuities $\dot{\mathbf{w}}$ are obtained adding the elastic term $\dot{\mathbf{w}}^e$ to the previous ones:

$$\left. \begin{array}{l} \mathbf{w} = \mathbf{w}^e + \mathbf{w}^i \\ \mathbf{w}^i = \mathbf{w}^p + \mathbf{w}^f \end{array} \right\} \Rightarrow \mathbf{w} = \mathbf{w}^e + \mathbf{w}^p + \mathbf{w}^f \quad (7)$$

The distinction between the two inelastic terms is motivated by the considered deterioration of the elastic stiffness in tension due to the damage parameter D : \mathbf{w}^f enters explicitly in the expression of D , while \mathbf{w}^p does not. The matrix of initial elastic stiffness coefficients \mathbf{K}_0 is diagonal with K_{n0} and K_{t0} defined as normal and tangential components respectively. An elastic deterioration coefficient ρ is introduced; ρ is fixed to one in compression, while it ranges from one to zero in tension according to the level of damage D :

$$\rho = 1 - \frac{\langle p_n \rangle}{|p_n|} D \quad (8)$$

where the symbol $\langle \bullet \rangle$ indicates the Macaulay brackets:

$$\langle \bullet \rangle = (\bullet + |\bullet|) / 2 \quad (9)$$

The traction – displacement discontinuity relationship reads:

$$\dot{\mathbf{p}} = \rho \mathbf{K}_0 (\dot{\mathbf{w}} - \dot{\mathbf{w}}^p) \quad (10)$$

Damage D can hence be defined as the complement to one of the ratio between the current normal stiffness K_{nc} and the initial one K_{n0} .

$$D = 1 - \frac{K_{nc}}{K_{n0}} = \frac{K_{n0} - K_{nc}}{K_{n0}} \quad (11)$$

It can be shown, (Červenka et al. 1998), that D is related to the current normal strength $\chi(w^{\text{ieff}})$ by the relationship:

$$D = 1 - \frac{\chi(w^{\text{ieff}})}{\chi(w^{\text{ieff}}) + (1 - \gamma) w^{\text{ieff}} K_{n0}} \quad (12)$$

where γ , a new parameter, is introduced to define the irrecoverable (plastic) portion of inelastic displacements:

$$w_n^p = \gamma w_n^i \quad (13)$$

Finally, the direction of inelastic displacements is explicitly defined by the gradient of the potential Q :

$$\dot{\mathbf{w}}^i = \frac{\partial Q}{\partial \mathbf{p}} \dot{\lambda} \quad , \quad \dot{\lambda} \geq 0 \quad (14)$$

$$\frac{\partial Q}{\partial \mathbf{p}} = \begin{cases} \begin{bmatrix} p_n/K_{n0} \\ p_t/K_{t0} \end{bmatrix} & \text{if } \frac{p_n}{|p_t|} \geq \mu_d \frac{K_{n0}}{K_{t0}} \\ \begin{bmatrix} |p_t| \mu_d \\ p_t \end{bmatrix} & \text{otherwise} \end{cases} \quad (15)$$

where μ_d is the dilatancy angle.

Around the origin of the stress space the inelastic return direction is toward the origin if $K_{n0} = K_{t0}$, otherwise it is given by the normal to an ellipse with aspect ratio $\sqrt{K_{t0}/K_{n0}}$; when the tangent to the ellipse equals the tangent μ_d of the dilatancy angle, the direction remains constant for every smaller value of normal traction p_n . However, for $w^{\text{ieff}} \leq w_{dil}$ the dilatancy μ_d is not constant but decreases linearly with w^{ieff} from its initial value μ_{d0} to zero:

$$\mu_d(w^{\text{ieff}}) = \begin{cases} \mu_{d0} (1 - w^{\text{ieff}}/w_{dil}) & w^{\text{ieff}} \leq w_{dil} \\ 0 & w^{\text{ieff}} > w_{dil} \end{cases} \quad (16)$$

Proposed extension to cyclic loading

This section presents an extension of the previously described interface model into a generalized one which can also capture the essential characteristics of joint cyclic behavior. This is done preserving the inherent capabilities of the original element, and maintaining its fracture mechanics based origin.

The cyclic model description presented herein is limited to those features that will be added or modified to the original Červenka model, namely: 1) introduction of an asperity function which characterizes joint roughness and governs the dilatancy of the model; 2) consideration of an integrity factor which keeps track of the degradation of the asperities; 3) modification of the yield function, of the friction angle in particular, to account for the sliding along inclined asperities.

Some other aspects of the response of joints to cyclic loading were not considered here for the following reasons:

1. Joint bulking or seating, that is the increase or decrease of joint thickness with asperity degradation respectively, was not included due to apparent lack of consistent experimental results.
2. Configuration rearrangements of third body granular layer particles caused by debris inside the joint (Stupkiewicz and Mróz 2001) is not accounted for due to: its minor relevance in the present context; complexity; paucity of experimental results.
3. Dilatancy associated to second order asperities has been deemed as not essential for the aims of the present model, though it would be easy to insert it in the model and despite the fact that Lee et al. (2001) and Jafari et al. (2003) report their influence on first loading cycles and for tangential relative displacements of small amplitude.
4. Asperity degradation caused by pure compressive stresses was left since it was preferred to describe permanent normal deformations by means of the elasto-plastic strains developing in the bulk material.
5. A fully 3D formulation, including effects such as anisotropic wear, has not been dealt with so far, but represents an important extension and possible subject of future work.

Analytical formulation

In what follows, the symbol α refers to quantities related to first order asperities, while β refers to all joint properties not related to first order asperities (such as tensile strength and cohesion) besides frictional quantities. The term “basic” will indicate joint properties associated with second order roughness, while “apparent” will refer to both orders.

Asperity definition

Following the formulation of Plesha (1987), and of Stupkiewicz and Mróz (2001), an asperity curve characterizing first order joint roughness can be defined as follows:

$$w_n^i = f(p_n, L_t^i) \cdot y(w_t^i) \quad (17)$$

This has to be intended as an average geometry of the joint surface reflecting the macroscopic (overall) behaviour of the joint rather than its microscopic structure as in (Fox et al. 1998), (Grasselli et al. 2002), Misra (2002). The asperity curve relates the joint irreversible normal (w_n^i) and tangential (w_t^i) relative displacements, and it is the product of the geometric curve y defining the initial asperity shape with an integrity parameter f (to be defined later) which reflects the joint degradation level and ranges from 1 to 0. Integrity (f) is assumed to be a function of normal traction p_n and tangential inelastic shear work L_t^i defined as follows in rate form:

$$\dot{L}_t^i = p_t \cdot \dot{w}_t^i \quad (18)$$

It should be noted that roughness degradation affects the asperity height only, while its wavelength remains unchanged.

In this work two particular asperity curves are considered, namely a Gaussian and a hyperbolic one:

$$y(w_t^i) = h_0 \left(1 - \exp\left(-\frac{1}{2} \left(\frac{w_t^i}{s}\right)^2\right) \right) \quad \text{Gaussian} \quad (19)$$

$$y(w_t^i) = \mu_{\bar{\alpha}0} \left(\sqrt{(w_t^i)^2 + (r_0 \mu_{\bar{\alpha}0})^2} - r_0 \mu_{\bar{\alpha}0} \right) \quad \text{hyperbolic} \quad (20)$$

The gaussian asperity function reaches a constant value for large sliding displacements, thus implying that asperities are not periodic so that dilatancy cannot be recovered once sliding has exceeded a characteristic asperity length. Figure 1(a) shows the two parameters of the Gaussian asperity curve: asperity height h_0 and asperity length ℓ_0 . Parameter s in equation 19 determines the curve amplitude and is therefore closely connected to ℓ_0 .

The evolution of the Gaussian asperity curve with progressive degradation is shown in fig. 1(a). Again it can be noted that only the ordinate (asperity height) is affected and not the abscissa (asperity length).

The hyperbolic asperity function, figure 1(b), grows indefinitely, even for large sliding displacements; therefore it is only appropriate for problems in which it is a priori known or assumed that the tangential slip w_t^i will be smaller than a characteristic asperity length. This curve is characterized by two parameters: the inclination angle of the asymptote of the hyperbola, $\bar{\alpha}_0$, and the curvature r_0 at the origin. The tangent of $\bar{\alpha}_0$ is named $\mu_{\bar{\alpha}0}$, according to the rule $\mu_x = \tan(x)$; $\bar{\alpha}_0$ is also the maximum value the asperity angle can attain for hyperbolic asperities. The same symbol will be used to indicate the

$$\bar{\alpha}_0 = h_0/s \cdot \exp(-1/2) \quad (21)$$

Saw-tooth shaped asperities, often adopted in roughness description, were not used for experimental and numerical reasons. As observed by (Hutson and Dowding 1990) and (Sun, Gerrard and Stephansson 1985), an initial amount of joint shearing is necessary to induce maximum dilatancy angle and shear strength. Besides, a curve with continuous derivative is computationally preferable.

Following (Stupkiewicz and Mróz 2001), the dilatancy curve introduced by equation 17 is used to explicitly prescribe the joint dilatant behavior as a function of current normal stress, inelastic tangential work and displacement.

Plesha (1987), Giambanco and Di Gati (1997) and other researchers have preferred to prescribe the dilatancy angle, instead of the dilatant displacement, as a function of current tractions, relative displacements and internal variables, but it was realized that this approach can lead to undesirable and uncontrollable joint bulking.

The dilatancy angle α_{dil} , shown in figure 1(b), is defined as the total variation of w_n^i with respect to w_t^i ; therefore, from equation 17:

$$\mu_{\alpha_{dil}} = \tan(\alpha_{dil}) = \frac{dw_n^i}{dw_t^i} = \frac{d(f y)}{dw_t^i} \quad (22)$$

Finally we have to consider that the effect of the asperity curve requires a modification to Červenka's flow rule, which defines the direction of the vector of inelastic displacement discontinuity. This direction is now defined such that under backward slip the joint does not dilate but contracts, figure 2(a). Hence, the gradient of the plastic potential Q is given by

$$\frac{\partial Q}{\partial \mathbf{p}} = \begin{cases} \begin{bmatrix} p_n/K_{n0} \\ p_t/K_{t0} \end{bmatrix} & \text{if } p_n \geq \mu_{\alpha_{dil}} \frac{K_{n0}}{K_{t0}} p_t \\ \begin{bmatrix} p_t \mu_{\alpha_{dil}} \\ p_t \end{bmatrix} & \text{otherwise} \end{cases} \quad (23)$$

Relationships 23 imply that the original formulation is retained under monotonic loading.

Asperity degradation

The integrity parameter f , introduced in equation 17 ranges from 1 to 0 and governs asperity degradation. The results of the experimental tests carried out by Lee et al. (2001), Homand et al. (2001), Jafari et al.

(2003), Huang, Haimson, Plesha and Qiu (1993) suggest that f will depend not only on the inelastic shear work L_t^i , as proposed by Plesha (1987) and Hutson and Dowding (1990), but also on the normal traction p_n . In fact:

- a non zero steady state asperity degradation of joints is reached after several shearing cycles at constant confinement.
- the residual, alias asymptotic, degradation depends on the amount of applied compressive stress.

The incremental expression of f is defined in terms of \bar{f} (integrity factor in the known configuration), p_n (normal traction in the ensuing state) and ΔL_t^i (increment of inelastic shear work between the two configurations) as follows :

$$\Delta f(\bar{f}, p_n, \Delta L_t^i) = \langle \bar{f} - f_{asym}(p_n) \rangle \cdot (1 - \exp(-C \Delta L_t^i)) \quad (24)$$

$$f_{asym}(p_n) = (-d p_n + 1)^{-1} \quad (25)$$

where, once again, the symbol $\langle \bullet \rangle$ indicates the Macaulay brackets (see eq. 9).

The asymptotic degradation factor f_{asym} provides a residual value under constant confinement when the increment of inelastic shear work ΔL_t^i tends to infinity.

Under tension the asperities are not worn and f_{asym} is fixed to 1; under increased compressive stress the asymptotic degradation factor decreases, reaching zero when p_n tends to minus infinity. Function $f_{asym}(p_n)$ is a hyperbola with a single parameter, d , which controls the speed rate as the function approaches zero. Its expression is relatively simple due to its derivation from qualitative, though not quantitative, experimental observations.

Looking at equation 24, it can be noted that for $\Delta L_t^i = 0$, that is if no tangential inelastic work takes place, then f is equal to \bar{f} for any value of p_n . Furthermore, asperities do not wear when $f_{asym}(p_n)$ is larger than \bar{f} , that is when asperities have already degraded more than they would under the current value of normal stress p_n for any value of ΔL_t^i .

Conversely, if $f_{asym}(p_n)$ is smaller than \bar{f} and p_n is kept constant, the integrity factor f decreases exponentially for increasing ΔL_t^i from \bar{f} to $f_{asym}(p_n)$. The speed of the exponential decay is controlled by C .

The evolution of f is defined by its gradient with respect to L_t^i and p_n :

$$\frac{\partial f}{\partial L_t^i} = - \langle \bar{f} - f_{asym}(p_n) \rangle \cdot C \quad (26)$$

$$\frac{\partial f}{\partial p_n} = 0 \quad (27)$$

where \bar{f} is again the current value of f .

Rotated activation function

The total variation of w_n^i with respect to w_t^i reads:

$$\frac{dw_n^i}{dw_t^i} = \left(\frac{\partial f}{\partial p_n} \cdot \frac{\partial p_n}{\partial w_t^i} + \frac{\partial f}{\partial L_t^i} \cdot p_t \right) \cdot y(w_t^i) + f \frac{\partial y}{\partial w_t^i} \quad (28)$$

Substituting equations 26 and 27 in 28, we note that the total derivative is contributed by a compaction and a friction term:

$$\frac{dw_n^i}{dw_t^i} = (-\langle \bar{f} - f_{asym}(p_n) \rangle \cdot C p_t) \cdot y(w_t^i) + f \frac{\partial y}{\partial w_t^i} \quad (29)$$

Only the frictional term is retained here to account for inclination of the sliding plane with respect to the joint mid-plane. Hence, the angle α , shown in figure 1(b), by which the yield function is rotated with respect to the original configuration is given by:

$$\alpha = \arctan(\mu_\alpha) = \arctan\left(f \frac{\partial y}{\partial w_t^i}\right) \quad (30)$$

For the Gaussian and hyperbolic asperity curves introduced in equations 19 and 20, the expression of μ_α reads:

$$\mu_\alpha = \frac{f h_0}{s^2} w_t^i \exp\left(-\frac{1}{2} \left(\frac{w_t^i}{s}\right)^2\right) \quad \text{Gaussian} \quad (31)$$

$$\mu_\alpha = f \mu_{\bar{\alpha}0} \left(\frac{w_t^i}{\sqrt{(w_t^i)^2 + (r_0 \mu_{\bar{\alpha}0})^2}} \right) \quad \text{hyperbolic} \quad (32)$$

The last modification which has to be introduced in Červenka model referd to the expression of the activation function for the inelastic displacement discontinuities.

In the model of Plesha (1987), the activation function φ is written in terms of local tractions transferred along inclined asperities. Expressing φ in the joint reference system corresponds to rotating the activation function by an angle α . In the current proposal the hyperbolic activation function of Červenka's model is modified through the rotation of its asymptotes, thus modifying the current (or apparent) friction angle. In this way an asymmetric activation function is obtained, composed of two branches of hyperbola with the same vertex (the tensile strength), but different inclination of the asymptotes.

Recalling that α represents the current slope of the asperity curve and β the basic friction angle (related to second order asperities), we can define the friction coefficients $\mu_{\beta+\alpha}$ and $\mu_{\beta-\alpha}$ in forward and

backward slip, respectively, as follows:

$$\mu_{\beta+\alpha} = \tan(\beta + \alpha) \quad (33)$$

$$\mu_{\beta-\alpha} = \tan(\beta - \alpha) \quad (34)$$

Because of the asymptote rotation, the apparent cohesion is modified:

$$c = \begin{cases} \frac{c_\beta}{\mu_\beta} \mu_{\beta+\alpha} & \text{forward slip} \\ \frac{c_\beta}{\mu_\beta} \mu_{\beta-\alpha} & \text{backward slip} \end{cases} \quad (35)$$

Apparent cohesion c depends on basic cohesion c_β and on the asperity angle α . This, often overlooked, dependency of the cohesion on the asperity angle is recognized in Fed (1999).

On the contrary, the tensile strength is not affected by the presence of first order asperities:

$$\chi = \chi_\beta \quad (36)$$

The hyperbolic activation function with rotated asymptotes is shown in figure 2(b). Its analytical expression is given by:

$$\varphi = \begin{cases} \left(\frac{\mu_\beta}{\mu_{\beta+\alpha}} \right)^2 p_t^2 - (c_\beta - p_n \mu_\beta)^2 + (c_\beta - \chi_\beta \mu_\beta)^2 & \forall p_t \geq 0 \\ \left(\frac{\mu_\beta}{\mu_{\beta-\alpha}} \right)^2 p_t^2 - (c_\beta - p_n \mu_\beta)^2 + (c_\beta - \chi_\beta \mu_\beta)^2 & \forall p_t < 0 \end{cases} \quad (37)$$

It can be observed that the proposed expression of φ has no meaning for $\alpha < \beta$. Moreover, if α is larger than β the inelastic work can have negative increments. Hence, the maximum slope of the asperity curve must satisfy the condition $\alpha < \beta$.

Remarks

In the presented extension of Červenka's model most terms retain their original meaning (such as damage D , inelastic effective displacement w^{ieff}), the main difference being that the bilinear softening law for cohesion now applies to c_β rather than to the apparent (or perceived) cohesion c .

Four new independent parameters have been introduced to the original model: two related to the asperity curve (initial asperity length ℓ_0 and initial asperity height h_0); two others modelling the asperity degradation (C and d). At the same time, however, two parameters of the monotonic version of Červenka's model have been discarded: the initial dilatancy angle μ_{d0} and the amount of effective inelastic displacement w_{dil} for which dilatancy μ_d reaches zero. These are now related to the chosen

asperity representation.

Computational tests

The predictive capabilities of the enhanced model introduced in the previous sections are shown here by comparison with the results of Kutter and Weissbach (1980) experimental test. Comparison with the predictions of the original Červenka formulation allows to lighten the improvements here proposed.

Comparison with Kutter and Weissbach test

The Kutter and Weissbach (1980) experimental results obtained from the *IALAD Network for the Integrity Assessment of Large Dams* (2004) web page are considered in which a cyclic slip was imposed under a constant compressive stress of 2.5MPa. The test, as described in (Plesha 1987), was performed on a joint in sandstone which was artificially produced by line loading. The specimen was 495 cm² in size.

The cyclic model with hyperbolic asperities has been used. Material parameters are selected in order to produce the best fit. The normal and tangential stiffness K_{n0} and K_{t0} equal 8.26 and 50 MPa/mm respectively. The friction angle β is 34.62 degrees, hence μ_β is 0.69. No tensile strength is assumed, while c_β amounts to 1.42 MPa and decreases linearly with w^{ieff} , hence only one additional parameter, namely fracture energy $G_f^{\text{II}a} = 15.57\text{MPa}mm$, is required. As for the asperities, the curvature radius r_0 is 38.86 mm and the angle $\bar{\alpha}_0$ is 10.85 degrees, i.e. $\mu_{\bar{\alpha}_0} = 0.192$. The asymptotic degradation parameter d is given a fairly large value so that complete degradation is possible under the imposed normal stress. However, since results at only one confinement are taken into account, the role of d is not so relevant in this analysis. Parameter C governing rate of asperity degradation with inelastic shear work is assumed to be 1.5 m/MN, a rather typical value. The tests of Kutter and Weissbach do not seem to start from an initially mated position, hence an initial inelastic tangential displacement of -2.5 mm is adopted.

The comparison of the two shear strength responses is in figure 3(a). The overall result is good, though some differences in shear strength degradation can be noticed, especially for positive shear displacements. The main difference is however in the initial stiffness, which is much lower in the experiment because, as mentioned, the joint is not fully in contact. This feature is not accounted for by the model.

The comparison between the cyclic model and experimental result's dilatancy is in figure 3(b). As can be seen the essential features of the response are reasonably well captured, however this figure is also good to highlight some of the already mentioned limitations of the model. In fact seating is not accounted for, nor is a possible different inclination of left and right asperities. The rate of first order asperities' degradation differs from the experimental one too. Maybe the inclusion of the dilatancy associated to second order asperities could improve the results, especially in the first cycle.

Anyway the asperity slope and curvature, and the initial offset (first sliding of the joint is accompanied by a slight contraction) are satisfactorily described by the model.

To summarize, this test well exemplifies capabilities and possible deficiencies of the proposed model. It should be noted that, though the model extension concerns precisely the cyclic shear behavior, the simulation of all cycles of Kutter and Weissbach test is a fairly exigent task.

Comparison with Červenka's model

The cyclic model results in Kutter and Weissbach (1980) experiment are now compared with Červenka's model response under the same loading conditions. To this end the latter model parameters are aptly chosen. Cohesion $c_0 = 2.01\text{MPa}$ includes the contribution of asperities and is thus obtained from the cyclic model parameters multiplying c_β by the factor $\tan(\beta + \bar{\alpha}_0) / \tan(\beta) = 1.47$ similarly to equation 35. Fracture energy $G_f^{IIa} = 22.93\text{MPa}\text{mm}$ is obtained amplifying G_f^{IIa} of the cyclic model by the same coefficient. Dilatancy $\mu_{d0} = 0.149$ is smaller than $\mu_{\bar{\alpha}0}$ to account for asperity curvature. It is obtained averaging μ_α between 0 and 29.1mm, i.e. the shear displacement at which the first inversion of sliding occurs in Kutter and Weissbach (1980) experiment. Parameter w_{dil} is obtained imposing that the residual integrity of the asperities is equal for the two models at the end of the test, alias $\mu_d / \mu_{d0} = f$. Friction coefficient μ equals μ_β . All other parameters have the same values of those adopted for the cyclic model.

The shear traction – shear displacement plot is displayed in figure 4(a). First of all, it can be noticed how Červenka's model reliably conveys the two most important pieces of information: the peak load and the average shear strength. However, the main feature of Červenka model response is that, once cohesion softening is completed, shear strength is constant irrespective of amount and direction of sliding displacement, i.e. of the characteristics of surface roughness and their degradation. Another difference between the models is in the shear displacement at which peak load is attained: smaller for Červenka that mobilizes instantaneously the maximum dilatancy angle; larger, and nearer to the experimental value, for the cyclic model in which asperity inclination α grows gradually with sliding w_t^i .

Looking at the dilatancy plot in figure 4(b) , a striking discrepancy can be noted in the amount of predicted joint opening. In fact, despite the apt choice of model parameters, Červenka's model response is quantitatively (almost one order of magnitude) and qualitatively incorrect. Unfortunately this overestimation is also unsafe because it induces a greater normal stress in the surrounding material which in turn allows for larger shear stresses to be transferred across the joint.

The reason for this wrong prediction is the constant sign of dilatancy as sliding direction is inverted. More deeply the cause lies in the almost independent description of shear stress and dilatancy phenomena which are in the cyclic model tightly connected through the asperity description. Indeed the importance of this aspect goes beyond the mere improvement in the modelling of cyclic shear tests.

Finally it should be remarked how the shortcoming of Červenka's model in figure 4(b) is customarily common to all mixed mode quasi brittle joint models devised originally for monotonic analysis, and how a close comparison has been possible in this case due to the similarity of the two models.

Conclusions

A general interface model has been formulated for reproducing the mechanical behavior of joints and cracks in quasi-brittle concrete-like materials under cyclic loading.

The model combines, and enhances, two existing ones: 1) a fracture mechanics based model proposed by Červenka et al. (1998) for concrete cracks, which accounts for loss of tensile strength and normal stiffness in mode I, and for friction and decrease of cohesion in mode II; and 2) an asperity based frictional model proposed by (Plesha 1987) for rough rock joints, which properly models configuration dependent dilation and shear strength of rough joints under cyclic loading conditions.

Numerical simulation of Kutter and Weissbach (1980) experimental tests exhibits encouraging results and provides a useful test to show the model capabilities, while comparison with the (Červenka et al. 1998) model response highlights the extent of the introduced novelties.

The proposed model, suitable for implementation in finite element codes based on either discrete or smeared interpretation of crack, integrates coherently a number of different basic mechanical processes as required by its sought application to dam engineering.

Acknowledgements

This work was largely made possible through the financial support of the Italian Ministry for University and Research (MIUR) which enabled the visit of V.E. Saouma to the Politecnico, along with the accompanying research fund. In addition, the first and second authors would like to acknowledge the support by MIUR through COFIN02 grant on "Concrete dam-foundation-reservoir systems: integrity assessments allowing for interactions".

References

- Ahmadi, M., Izadinia, M. and Bachmann, H.: 2001, A discrete crack joint model for nonlinear dynamic analysis of concrete arch dam, *Computers & Structures* **79**, 403–420.
- Bažant, Z. P. and Gambarova, P.: 1980, Rough cracks in reinforced concrete, *Journal of the Structural Division* ASCE **106**(ST4), 819–842.
- Carol, I., Prat, P. C. and López, C. M.: 1997, Normal/shear cracking model: Application to discrete crack analysis, *J. Engng. Mech. Div.*, ASCE **123**(8), 765–773.
- Cocchetti, G., Maier, G. and Shen, X.: 2002, Piecewise linear models for interfaces and mixed mode cohesive cracks, *Computer Modelling in Engineering & Sciences* **3**, 279–298.
- Divoux, P., Boulon, M. and Bourdarot, E.: 1997, A mechanical constitutive model for rock and concrete joints under cyclic loading, in Rossmanith (ed.), *Damage and Failure of Interfaces*, Rotterdam, Balkema, pp. 443–450.
- Divoux, P., Bourdarot, E. and Boulon, M.: 1997, Use of joint elements in the behaviour analysis of arch dams, in Pietruszczak and Pande (eds), *Numerical Models in Geomechanics*, Rotterdam, Balkema, pp. 569–574.
- Fed: 1999, *Engineering Guidelines for the Evaluation of Hydropower Projects*.
- Fenves, G. L., Mojtahedi, S. and Reimer, R. B.: 1992, Parameter study of joint opening effects on earthquake response of arch dams, *Technical Report 92/05*, Earthquake Engineering Research Center - University of California at Berkeley.
- Fox, D. J., Kana, D. D. and Hsiung, S. M.: 1998, Influence of interface roughness on dynamic shear behavior in jointed rock, *Int. J. Rock Mech. Min. Sci.* **35**(7), 923–940.
- Fronteddu, L., Léger, P. and Tinawi, R.: 1998, Static and dynamic behaviour of concrete lift joint interfaces, *Journal of Structural Engineering*, ASCE **124**(12), 1418–1430.
- Giambanco, G. and Di Gati, L.: 1997, A cohesive interface model for the structural mechanics of block masonry, *Mechanics Research Communications* **24**(5), 503–512.
- Goodman, R., Taylor, R. and Brekke, T.: 1968, A Model for the Mechanics of Jointed Rocks, *J. Soil Mech. Div.*, ASCE **94**.
- Grasselli, G., Wirth, J. and Egger, P.: 2002, Quantitative three-dimensional description of a rough surface and parameter evolution with shearing, *Int. J. Rock Mech. Min. Sci.* **39**, 789–800.

- Hall, J. F.: 1998, Efficient non-linear seismic analysis of arch dams, *Earthquake Engng. Struct. Dyn.* **27**, 1425–1444.
- Hansen, E. and Saouma, V.: 2003, 3 d nonlinear finite element/fracture mechanics analysis of a pressurized nuclear reactor container ring, *Nuclear Engineering and Design* **225**, 1–10.
- Hohberg, J.-M.: 1992, *A joint element for the nonlinear dynamic analysis of arch dams*, PhD thesis, Institute of Structural Engineering, ETH, Zurich.
- Homand, F., Belem, T. and Souley, M.: 2001, Friction and degradation of rock joint surfaces under shear loads, *Int. J. Numer. Anal. Meth. Geomech.* **25**, 973–999.
- Huang, X., Haimson, B. C., Plesha, M. E. and Qiu, X.: 1993, An investigation of the mechanics of rock joints.—part I. laboratory investigation, *Int. J. Rock Mech. Min. Sci. & Geomech. Abstr.* **30**(3), 257–269.
- Hutson, R. and Dowding, C.: 1990, Joint asperity degradation during cyclic shear, *Int. J. Rock Mech. Min. Sci. & Geomech. Abstr.* **27**(2), 109–119.
- IALAD Network for the Integrity Assessment of Large Dams*: 2004, internet home page. <http://nw-ialad.uibk.ac.at>.
- Iesulauro, E., Ingraffea, A. R., Arwade, S. and Wawrzynek, P. A.: 2002, Simulation of grain boundary decohesion and crack initiation in aluminum microstructure models, *Fatigue and Fracture Mechanics: 33rd Volume, ASTM STP 1417*.
- Jafari, M., Hosseini, K. A., Pellet, F., Boulon, M. and Buzzi, O.: 2003, Evaluation of shear strength of rock joints subjected to cyclic loading, *Soil Dynamics and Earthquake Engineering* **23**, 619–630.
- Kutter, H. K. and Weissbach, G.: 1980, Der einfluss von verformungs- und belastungsgeschichte auf den scherwiderstand von gesteinskluften unter besonderer berucksichtigung der mylonitbildung., *Technical Report Research Project Ku 361/2/4*, DFG. in German.
- Lee, H. S., Park, Y. J., Cho, T. F. and You, K. H.: 2001, Influence of asperity degradation on the mechanical behavior of rough rock joints under cyclic shear loading, *Int. J. Rock Mech. Min. Sci.* **38**(7), 967–980.
- Lotfi, H. R. and Shing, P. B.: 1994, Interface model applied to fracture of masonry structures, *Journal of Structural Engineering*, ASCE **120**(1), 63–80.
- Misra, A.: 2002, Effect of asperity damage on shear behavior of single fracture, *Engineering Fracture Mechanics* **69**(17), 1997–2014.

- Mróz, Z. and Giambanco, G.: 1996, An interface model for analysis of deformation behaviour of discontinuities, *Int. J. Numer. Anal. Meth. Geomech.* **20**(1), 1–33.
- Patton, F.: 1966, *Multiple modes of shear failure in rock and related materials*, PhD thesis, University of Illinois.
- Paulay, T. and Loeber, T. J.: 1974, Shear transfer by aggregate interlock, *Shear in Reinforced Concrete*, Vol. 1 of *ACI Special Publication*, American Concrete Institute, Detroit, Michigan, pp. 1–16.
- Plesha, M. E.: 1987, Constitutive models for rock discontinuities with dilatancy and surface degradation, *Int. J. Numer. Anal. Meth. Geomech.* **11**(4), 345–362.
- Puntel, E.: 2004, *Experimental and numerical investigation of the monotonic and cyclic behaviour of concrete dam joints*, PhD thesis, Politecnico di Milano.
- Qiu, X., Plesha, M. E., Huang, X. and Haimson, B. C.: 1993, An investigation of the mechanics of rock joints.—part II. analytical investigation, *Int. J. Rock Mech. Min. Sci. & Geomech. Abstr.* **30**(3), 271–287.
- Saouma, V., Natekar, D. and Sbaizero, O.: 2002, Nonlinear finite element analysis and size effect study of a metal-reinforced ceramics-composite, *Materials Science and Engineering A* **323**, 129–137.
- Snyman, M. F. and Martin, J. B.: 1992, A consistent formulation of a dilatant interface element, *Int. J. Numer. Anal. Meth. Geomech.* **16**(7), 493–527.
- Stupkiewicz, S. and Mróz, Z.: 2001, Modelling of friction and dilatancy effects at brittle interfaces for monotonic and cyclic loading, *Journal of Theoretical and Applied Mechanics* **39**, 707–739.
- Sun, Z., Gerrard, C. and Stephansson, O.: 1985, Rock joint compliance tests for compression and shear loads, *Int. J. Rock Mech. Min. Sci. & Geomech. Abstr.* **22**(4), 197–213.
- Tassios, T. P. and Vintzēleou, E. N.: 1987, Concrete-to-concrete friction, *Journal of Structural Engineering*, ASCE **113**(4), 832–849.
- Červenka, J.: 1994, *Discrete crack modeling in concrete structures*, PhD thesis, University of Colorado, Boulder, Colorado.
- Červenka, J., Kishen, J. M. C. and Saouma, V. E.: 1998, Mixed mode fracture of cementitious bimaterial interfaces; part II: numerical simulation, *Engineering Fracture Mechanics* **60**(1), 95–107.

Notation

The following symbols are used in this paper:

Latin symbols

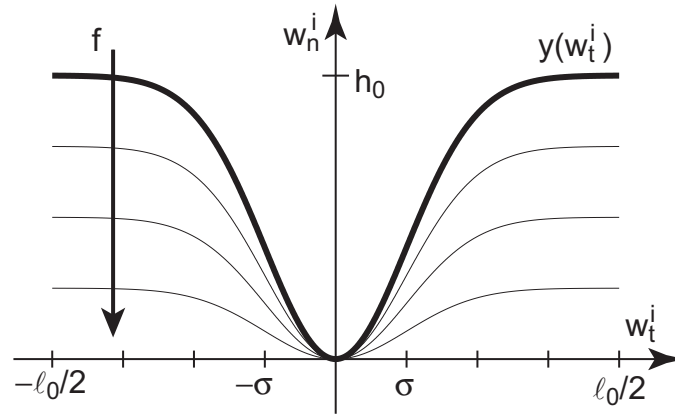
c	(apparent) cohesion
C	rate of asperity degradation due to inelastic tangential work
c_0	initial cohesion (bilinear softening law)
c_1	cohesion at break point (bilinear softening law)
c_β	joint cohesion in the absence of first order asperities
d	rate of decrease of f_{asym} for increasing compressive stress
D	joint damage in tension
f	asperity integrity (alias degradation) factor
f_{asym}	asymptotic asperity degradation factor (reached for $L_t^i \rightarrow \infty$)
\bar{f}	current value of asperity degradation factor f
G_f^I	mode I fracture energy (softening law)
G_f^{IIa}	mode II fracture energy at high confinement (softening law)
h	asperity height;
h_0	initial asperity height
\mathbf{K}_0	joint stiffness matrix (diagonal)
K_{n0}	initial normal stiffness
K_{nc}	current normal stiffness (degrades in tension)
K_{t0}	initial tangential stiffness
ℓ_0	initial asperity length
L	work
L_t^i	inelastic tangential work
\mathbf{p}	joint stress vector
Q	plastic potential
r	curvature radius in the origin (hyperbolic asperities)
r_0	initial value of curvature radius in the origin (hyperbolic asperities)
s	standard deviation (length) of gaussian asperities
\mathbf{w}	joint displacement discontinuity vector
w_{c0}	value of w^{ieff} at zero cohesion (bilinear softening law)
w_{c1}	value of w^{ieff} at cohesion breakpoint (bilinear softening law)
$w_{\chi 0}$	value of w^{ieff} at zero tensile strength (bilinear softening law)
$w_{\chi 1}$	value of w^{ieff} at tensile strength breakpoint (bilinear softening law)
w_{dil}	value of w^{ieff} at zero dilatancy (Červenka model only)
w^{ieff}	effective inelastic displacement discontinuity (softening variable)
w_n^i	normal inelastic displacement discontinuity
w_t^i	tangential inelastic displacement discontinuity
$y(w_t^i)$	function prescribing the initial asperity shape

Greek symbols

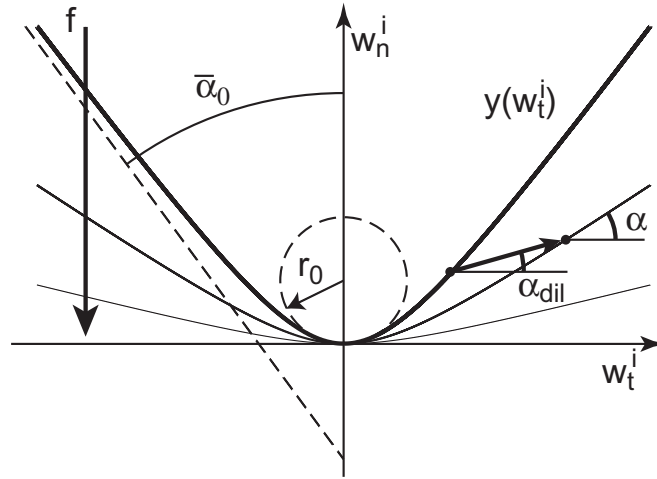
α	first order asperity angle
$\bar{\alpha}_0$	maximum asperity angle (gaussian and hyperbolic asperities)
	asymptotic asperity angle (hyperbolic asperities)
α_{dil}	dilatancy angle
β	second order asperity (friction) angle
γ	irrecoverable portion of total displacement in tension
χ_0	initial tensile strength (bilinear softening law)
χ_1	tensile strength at break point (bilinear softening law)
χ_β	joint tensile strength in the absence of first order asperities
φ	joint activation (alias yield) function
μ	friction coefficient (Červenka model only)
μ_d	tangent of the dilatancy angle (Červenka model only)
μ_{d0}	initial tangent of the dilatancy angle (Červenka model only)
ρ	stiffness reducing coefficient in tension

Contents

Introduction	2
Cyclic behavior of quasi brittle interfaces	4
Červenka 1994 hyperbolic model	5
Proposed extension to cyclic loading	7
Analytical formulation	8
Asperity definition	8
Asperity degradation	10
Rotated activation function	11
Remarks	13
Computational tests	13
Comparison with Kutter and Weissbach test	13
Comparison with Červenka's model	14
Conclusions	15
Acknowledgements	16
References	17
Notation	20

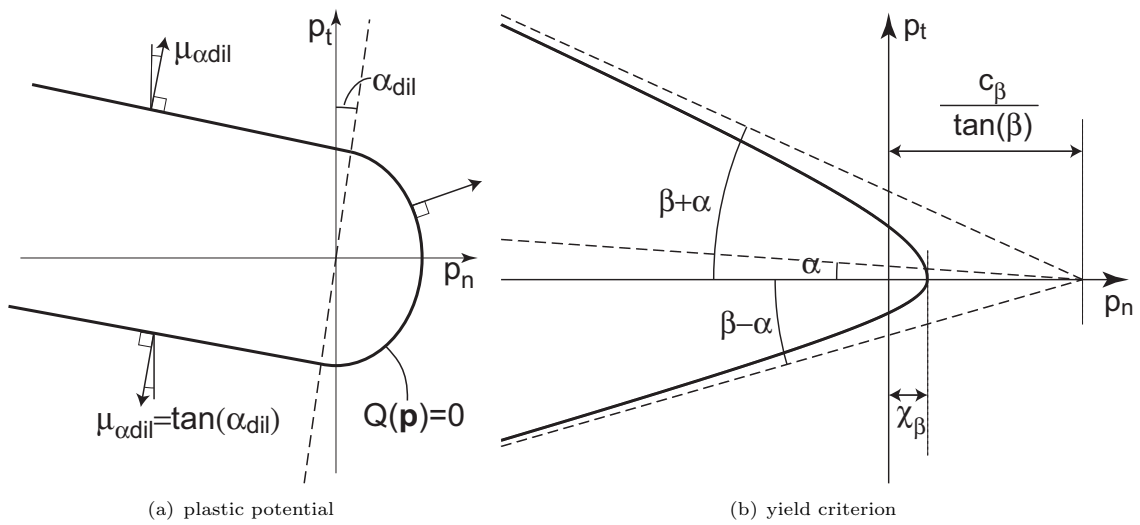


(a) Gaussian asperity curve



(b) Hyperbolic asperity curve and definition of angles α and α_{dil}

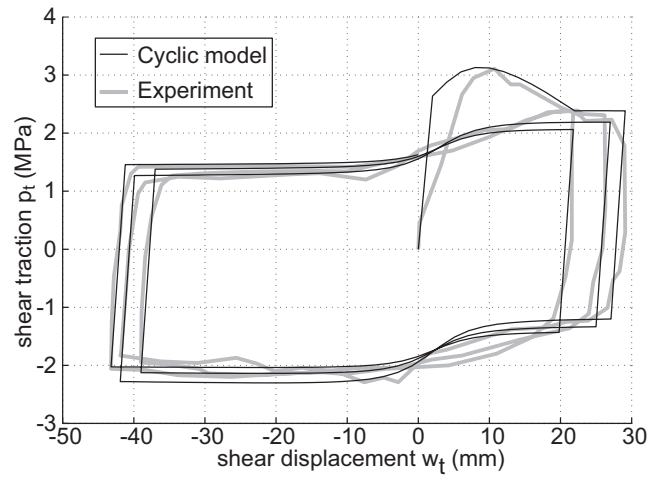
Figure 1: Asperity curves



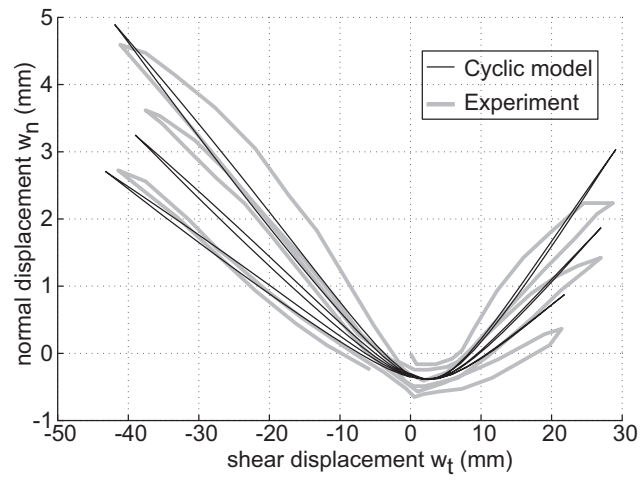
(a) plastic potential

(b) yield criterion

Figure 2: Cyclic model: yield criterion and plastic potential

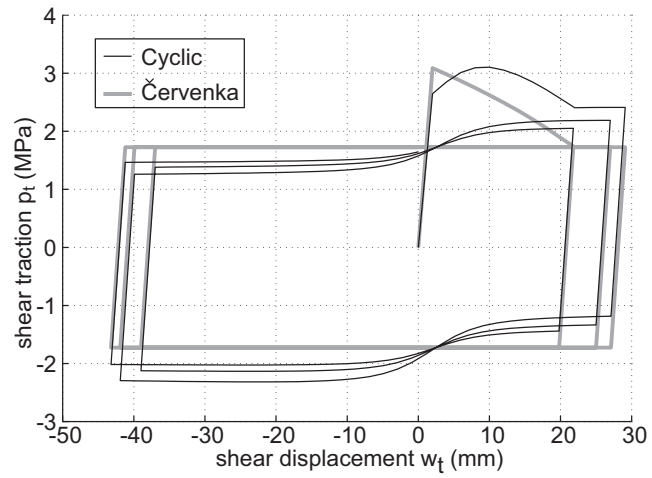


(a) shear strength

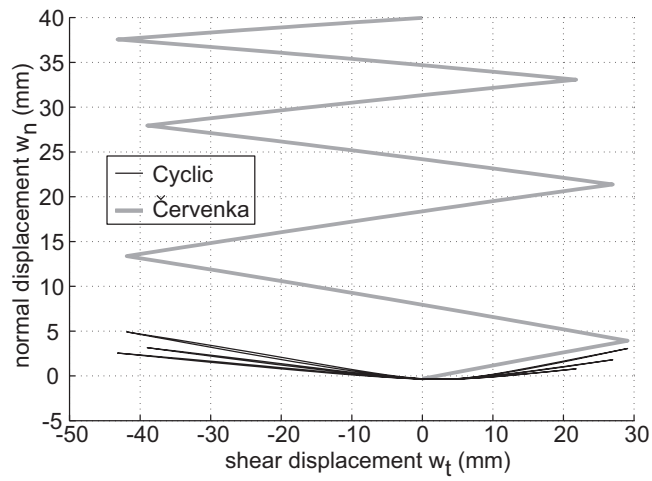


(b) dilatancy

Figure 3: Comparison with Kutter-Weissbach test results



(a) shear strength



(b) dilatancy

Figure 4: Červenka model vs. cyclic model